Proceedings of the Korean Nuclear Society Autumn Meeting
Seoul, Korea, October 1998

PIN POWER RECONSTRUCTION FROM THE HANARO FUEL ASSEMBLY GAMMA SCANNING

Chul Gyo Seo*, Chang Je Park, Nam Zin Cho
Korea Advanced Institute of Science and Technology

Hark Rho Kim
Korea Atomic Energy Research Institute

Abstract

To determine the pin power distribution without disassembling, HANARO fuel assemblies were gamma-scanned using the tomography method and then the pin power distribution is reconstructed by using numerical methods. The gamma rays emitted in proportion to the pin power distribution are measured by a NaI(Tl) detector rotating an assembly at every 10 degrees. The pin power distribution $\boldsymbol{x}=\{x_1, x_2, ..., x_m\}$ *and the measured counts* $\boldsymbol{b}$ *are related in a coupled set of equations as* $\boldsymbol{Ax}=\boldsymbol{b}$*. The elements in attenuation matrix* $\boldsymbol{A}$*, which give the possibility that a photon emitted from each pin will be detected by the detector, are calculated using the MCNP4B code.*

The iterative least squares method (ILSM) and the wavelet singular value decomposition method (WSVD) are chosen to solve this problem. An optimal convergence criterion is used to stop the iteration algorithm to overcome the divergence in ILSM. WSVD gives a little better results and is more stable than ILSM. The averaged values from two methods give the best results. The results show that it is possible to reconstruct the pin power distribution from the assembly gamma scanning without disassembling.

1. Introduction

It is very important to accurately predict the power distribution in a reactor in the viewpoint of reactor safety as well as operability. The accuracy of the predictions must be verified against the measured data. Usually, the gamma scanning method is used for measuring the power distribution. For measuring the pin power distribution, it is inevitable to disassemble the assemblies. Assemblies used in this measurement are almost fresh clean in the viewpoint of burnup. The fuel assembly is very expensive and it is very hard to reassemble the fuel assembly after disassembling. It takes very long time to measure each pin individually. If it is possible to measure the pin power distribution without disassembling, we can save time and cost. In this paper, we introduce a method to measure the pin power distribution without disassembling in HANARO and present some numerical results.

2. Experiment

During the nuclear commissioning of HANARO, the assemblies at fresh clean state were irradiated to measure the power distribution and the fast flux distribution.[1,2,3] The 1st core is loaded with sixteen 36-element fuel assemblies and eight 18-element

*Present Address : Korea Atomic Energy Research Institute

fuel assemblies as shown in Figure 1. The shaded sites are loaded with the fuel assemblies and the others are loaded with the dummy assemblies made of aluminum elements.

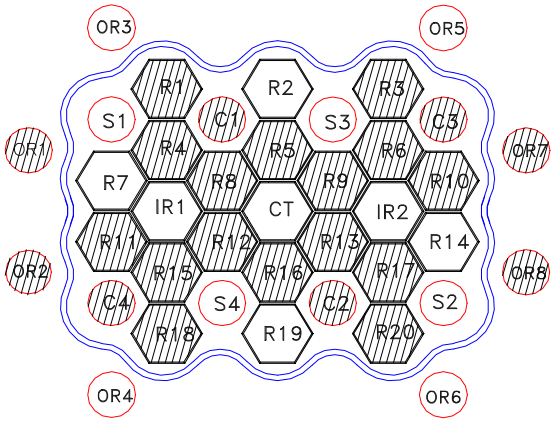

Figure 1. Loading Pattern of the 1st Core

To activate the assemblies properly, the reactor was operated for about 16 hours at 150 kW. And then sixteen 36-element assemblies were cooled for 3 months and used to measure the radial and axial power distributions by using the gamma scanning system at IMEF (Irradiation Material Experimental Facility). The gamma scanning system, which can move the bench axially 0.01mm at a step and rotate 0.01° at a step, is very precisely controlled by a PLC (Programmable Logic Controller). For this experiment, an assembly is put into an Al canister and water is filled to enlarge the attenuation differences of gamma rays emitted from each pin. And then it is located at the bench, which accepts a pin or an assembly, in the hotcell. The experimental setting is shown in Figure 2. In this experiment, the axial measuring position is at the axial peaking position of each assembly, namely 2-dimensional measurement.

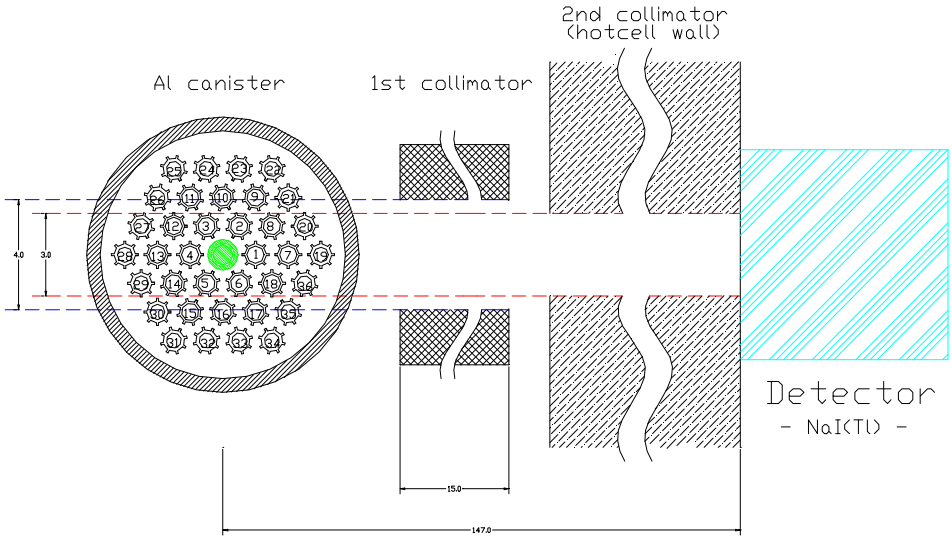

Figure 2. Plan View of the Experimental Setting

The starting point of the axial measuring position can be settled easily because the shielding is nearly perfect and the axial movement is controlled by 0.01mm at a step. The active length of the pin is 70cm and the gamma rays from fission products of the pins are observed only in the active range. At the axial measuring position, the

measurements are conducted as an assembly is rotating step by step at 10^{o} clockwise.

It is difficult to settle the angular starting point. The Al canister used in this experiment has a hexagonal shape at the lower part and a triangular groove inside. If the three triangular guides of the assembly are located at the triangular groove inside, the angular starting position can be settled using the hexagonal shape outside the Al canister. A viewer using a telescope can adjust exactly the angular starting position not to observe two opposite sides of the hexagonal shape as in Figure 3.

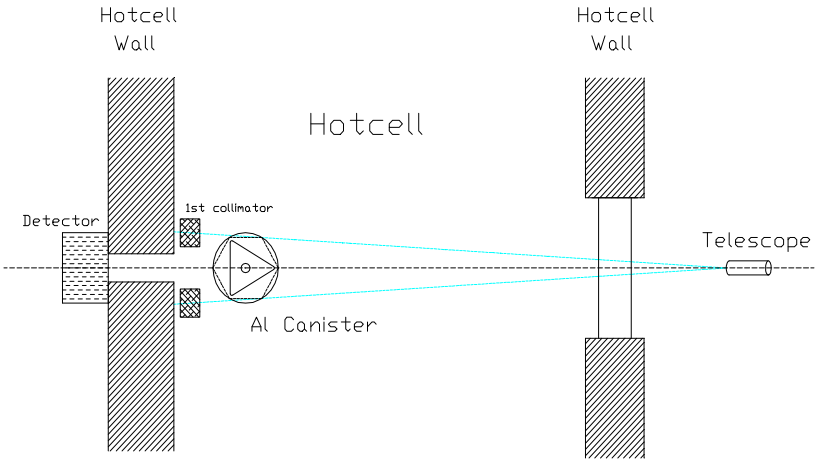

Figure 3. Schematic Diagram for Setting the Angular Starting Position

An HpGe detector is used to identify nuclides before starting the gamma scanning and then a NaI(Tl) detector is used to reduce the measuring time in all measurements. From the measurement using an HpGe detector, we select Zr-95 and Nb-95 as representative nuclides to measure the power distribution. In Figure 4, the spectra from NaI(Tl) and HpGe detectors are overlapped and a summed peak in the NaI(Tl) detector consists of 724.2(15%), 756.7(15%) and 765.8(70%) keV peaks in the HpGe detector.

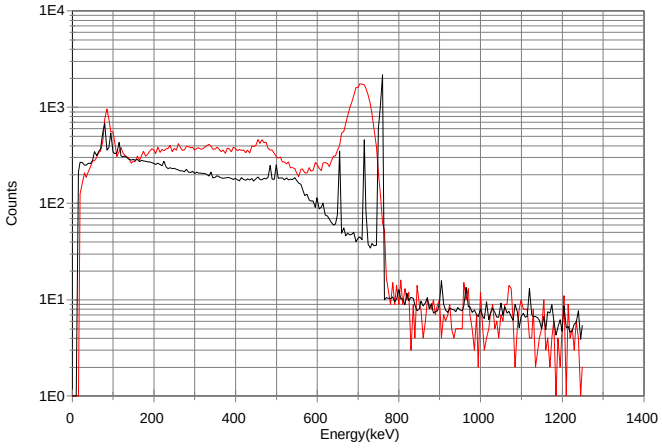

Figure 4. Spectra Measured Using HpGe & NaI(Tl)

Using a NaI(Tl) detector, the measurements to determine the pin power distribution were conducted for all sixteen 36-element assemblies while rotating the assembly by 10^{o}. Figure 5 shows the several measured results as an example.

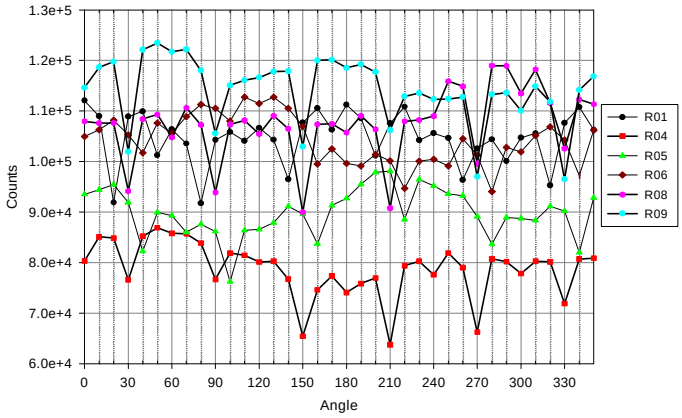

Figure 5. A Selection of Measured Results

The measured results show a peculiarity that the counts are lower at around 30° than other angular positions and repeated at every 60°. This phenomenon comes from the fact that the gamma rays are principally attenuated by pins and significantly attenuated when pins are arranged in row after row to the detector at a certain angle as in Figure 2. The measurements that the lower counts do not appear at 30° must be wrong. An assembly (R16) is measured by 2° for observing the sensitivity of measured counts to the angle as shown in Figure 6. From a comparison with the counts measured by 10°, it is confirmed that the measurement by 10° is deviated about 6° from the starting point. Thus the doubtful measurements are excluded and 5 cases, i.e., assemblies in R4, R8, R9, R10, R16 are used in this study.

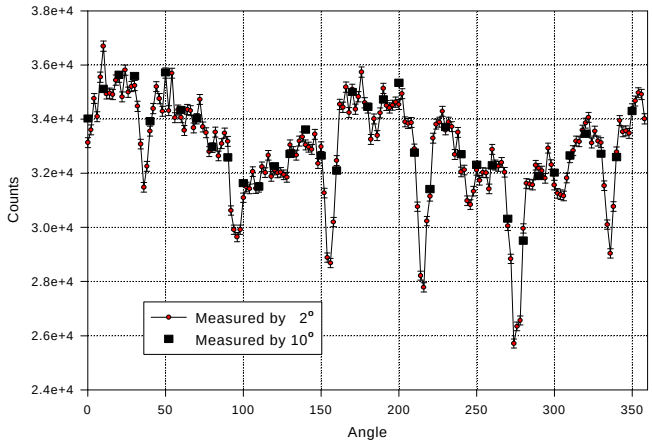

Figure 6. Angular Sensitivity of the Measured Counts

3. Analysis

The gamma rays counted at a detector are the summation of uncollided or not-attenuated gamma rays emitted from pins in proportion to the pin power distribution. Thus the measured photons are related with the pin power distribution. The pin power distribution $\boldsymbol{x}=\{x_1, x_2, \ldots, x_{36}\}$ and the measured counts $\boldsymbol{b}$ are related in a coupled set of equations as :

$$\sum_{i=1}^{36} a_{ij} x_i = b_j \quad \Rightarrow \quad \boldsymbol{Ax} = \boldsymbol{b}, \tag{1}$$

where b_j, a_{ij} and x_i represent the measured counts at angle j, attenuation factor of

pin i at angle j and power of pin i, respectively.

The attenuation factors a_{ij} mean the possibility that a photon emitted from each pin will be detected. The factors can be obtained by calculation or direct experiment, but it is very difficult to get the factors exactly. Although this equation seems to be a simple linear algebraic equation, it is difficult to solve because this equation formally requires the inversion of matrix $\boldsymbol{A}$, which introduce some errors. This inverse problem is notorious for being poorly conditioned. It is difficult because the experimental data $\boldsymbol{b}$ is insensitive to variation in a single unknown and the small errors in $\boldsymbol{A}$ is magnified to the large errors in $\boldsymbol{x}$.[4] But, if we get exact $\boldsymbol{A}$ and $\boldsymbol{b}$, we can obtain the pin power distribution exactly.

3.1 Calculation of Attenuation Factors

The factors can be directly obtained by experiments, but we get them by calculation to avoid disassembling and another experiment. We used the MCNP4B code, which can model complex geometry and has been validated to solve accurately various photon transport problems.[5,6] Fins in the cladding are approximated as cladding with equivalent diameter because the directions of fins are arbitrary. Since the detector is far from the source and uncollided photons are rare, the calculation efficiency is very low. The variance reduction technique used in the calculation is source biasing, which confines solid angle of the isotropic source to a fixed angle, within which photons are counted actually to the detector. The counts, $\boldsymbol{b}^c=\boldsymbol{A}\boldsymbol{x}^c$, calculated using the calculated attenuation matrix $\boldsymbol{A}$ and the pin power distribution $\boldsymbol{x}^c$ from the reactor calculation, are compared with the measurement $\boldsymbol{b}$ in Figure 7. Since we do not have the measured pin power data yet, the calculation results using MCNP are used as the reference data in this paper.

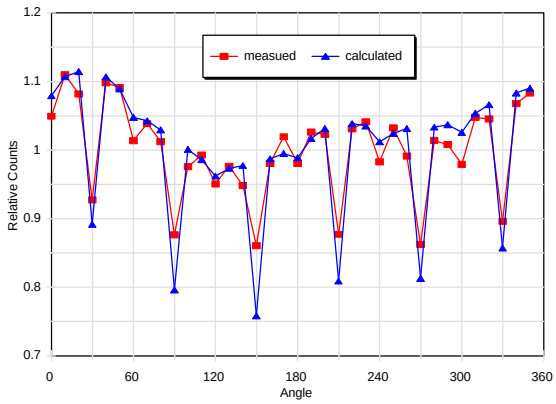

Figure 7. A Comparison of the Calculation with the Measurement

3.2 Numerical Methods

We tested many numerical methods for solving these problems. Most methods give unrealistic results because both $\boldsymbol{A}$ and $\boldsymbol{b}$ have errors. In this kind of inverse problems, the iterative least squares method has been well known for giving good results[7] and the wavelet singular value decomposition method becomes popular nowadays.[8,9]

Iterative Least Squares Method (ILSM)

The ILSM method is based on minimizing the relative difference R about a pin power $x_{i_o}^{n+1}$ between the measured counts b_j (with measurement error σ_j) and estimated counts c_j^n at the nth iteration in a least squares sense as follows :[7]

$$R(x_{i_o}^{n+1}) = \sum_j \frac{(b_j - c_j^n)^2}{\sigma_j^2} . \tag{2}$$

Solving for $x_{i_o}^{n+1}$, we get

$$x_{i_o}^{n+1} = x_{i_o}^n + \Delta^n x_{i_o} , \tag{3}$$

where $\Delta^n x_{i_o} = \left\{ \sum_j a_{ji_o} [b_j - c_j^n] / \sigma_j^2 \right\} / \sum_j (a_{ji_o}/\sigma_j)^2$.

But the solutions may not converge and could oscillate, so a damping factor δ is introduced. Again, using the concept of the least squares, we have the following equations :[7]

$$x_{i_o}^{n+1} = x_{i_o}^n + \delta \Delta^n x_{i_o} , \tag{4}$$

where

$$\begin{aligned} \Delta^n x_{i_o} &= \left\{ \sum_j a_{ji_o} [b_j - c_j^{n+1}] / \sigma_j^2 \right\} / \sum_j (a_{ji_o}/\sigma_j)^2 , \\ c_j^{n+1} &= \sum_i a_{ij} x_i^n , \\ \delta &= \frac{\sum_j (b_j - c_j^n) \left[\sum_i a_{ji} \Delta^n x_i \right] / \sigma_j^2}{\sum_j \left(\sum_i a_{ij} \Delta^n x_i \right)^2 / \sigma_j^2} . \end{aligned} \tag{5}$$

Wavelet Singular Value Decomposition Method (WSVD)

In WSVD, Eq. (1) is solved in wavelet transformed domain. We define the vectors :

$$\eta \equiv Wb, \qquad \xi \equiv Wx . \tag{6}$$

where W is matrix representation of 1-D wavelet transform.[10] From Eqs. (1) and (6), we have

$$\eta = \Gamma \xi , \tag{7}$$

where the multiscale system matrix Γ is given by

$$\Gamma = WA W^T . \tag{8}$$

Using the regularized least squares (RLS), the solution of Eq. (7) is given by

$$(\Gamma^T \Gamma + \lambda I) \hat{\xi} = \Gamma^T \eta , \tag{9}$$

where λ is a regularization parameter.
Eq. (9) is then solved using the SVD method to overcome the near-singularity in matrix Γ.

Uncertainty Analysis

The measurement $\boldsymbol{b}$ and the attenuation matrix $\boldsymbol{A}$ have some errors. So a sensitivity to the noise is studied. For the noise analysis, we consider white Gaussian noise in WSVD and ILSM. We add some noises to matrix $\boldsymbol{A}$ and vector $\boldsymbol{b}$, respectively. In case of no noise, the solutions of two methods are exact. Unlike WSVD, ILSM converges to an unrealistic solution at a small noise. So ILSM needs a stopping criterion to stop the iterations. Table I shows the root mean square error (RMSE) of WSVD and ISLM. The results indicate that WSVD has better robustness in noise contaminated problems.

Table I. RMSE of WSVD and ILSM* at Various Noise Levels

A \ *b*	0.005**	0.01	0.05
0.005	5.44 (5.86)***	5.35 (5.88)	9.09 (11.95)
0.01	5.41 (5.85)	5.33 (5.87)	9.08 (11.84)
0.05	5.61 (5.73)	5.55 (5.73)	9.29 (11.10)

* Stopping criteria : 1.0E-04
** Gaussian white noise level (σ)
*** RMSE(%) in WSVD (ILSM)

4. Results and Discussion

Since the solutions by ILSM converge to unrealistic values, the iterations must be stopped at a proper step. The RMSE and discrepancy versus iterations are shown in Figure 8. For optimally stopping the iterations, the discrepancy level is used and set to 0.1.

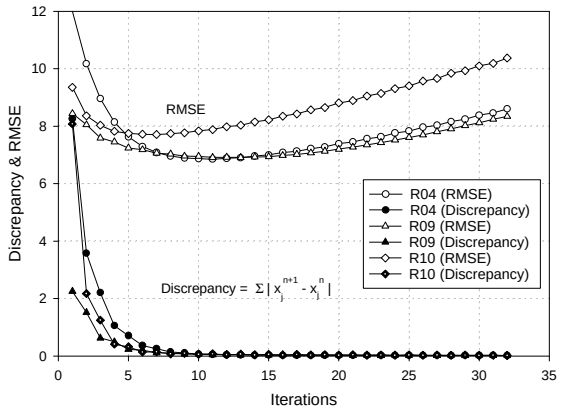

Figure 8. The Divergence of the Solutions by ILSM

Table II. Results of the Reconstruction Using WSVD and ILSM

Error / Case	RMSE(%)			Maximum Error(%)		
	WSVD	ILSM	Average	WSVD	ILSM	Average
R04	5.20	6.89	**5.13**	12.48	15.06	**10.15**
R08	8.35	8.25	**6.61**	13.90	19.85	**13.66**
R09	6.05	6.72	**4.98**	13.66	16.73	**12.15**
R10	7.63	7.93	**6.53**	17.67	14.20	**13.58**
R16	9.09	7.98	**6.44**	14.15	17.55	**14.30**

WSVD gives slightly better results and is more stable than ILSM as shown in Table II. The average values from these methods could be used because the two method are independent. Since the reference data calculated by MCNP have a statistical error 3% of the MCNP calculation itself,[1] the reconstructed results would be close to the real distribution. Figure 9 shows an example of the reconstruction results. The results show the feasibility of reconstruction of the pin power distribution from the assembly gamma scanning without disassembling.

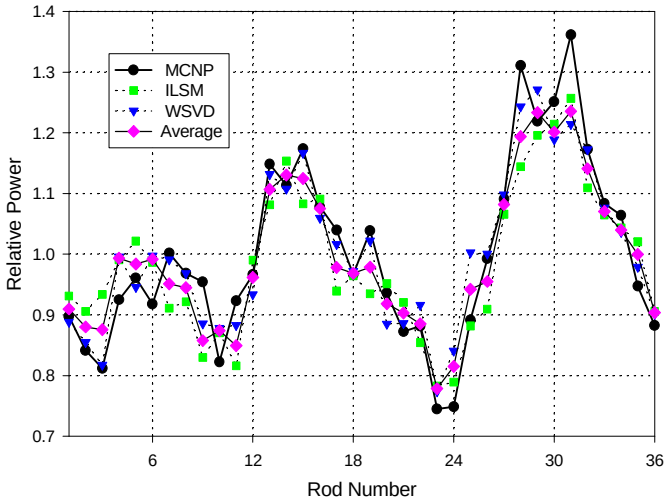

Figure 9. An Example of the Reconstruction Results

The divergence of the solutions by ILSM and the errors by WSVD come from the errors in the attenuation factors. This is inferred from the fact that the calculated results are always lower than the measured results at every lower positions in Figure 7. The attenuation factors are calculated assuming that the conditions such as the positions of pins and the angular directions are precise. Although the positions of pins are well positioned within a manufacturing tolerance, the attenuation factors are affected by a small deviation within the tolerance. The attenuation factors of the pins near the extended line of slit are sensitive. Also the measured counts are sensitive to the variation of a small angle as shown in Figure 6. Therefore, the accuracy of the angular starting point is important. If these parameters are considered properly, we will obtain more accurate results.

References

1. Chul Gyo Seo, "Assemblywise Power Distribution Measurement," *HANARO Commissioning Test Report, TP-RPT-C-08,* 1998.
2. Byung Chul Lee, "Fast Neutron Flux Measurement," *HANARO Commissioning Test Report, TP-RPT-C-07,* 1997.
3. Byung Chul Lee and Chul Gyo Seo, "Thermal and Fast Neutron Reaction Rates in HANARO," *Proceedings of The 5th Asian Symposium on Research Reactors,* **Vol. 1**, p.117, Taejon, Korea, May 29-31, 1996.
4. N. J. McCormick, "Inverse Radiative Transfer Problems: A Review," *Nuclear Science and Engineering,* **112**, p.185 (1992).
5. J. F. Briesmeister (Editor), "MCNP-A General Monte Carlo N-Particle Transport Code," LA-12625-M, Los Alamos National Lab. (1993).
6. D. J. Whalen, et al., "MCNP: Photon Benchmark Problems," LA-12196, 1991.
7. T. F. Budinger and G. T. Gullberg, "Three-Dimensional Reconstruction in Nuclear Medicine Emission Imaging," *IEEE Trans. Nucl. Sci.*, **NS-21**, 2-20, June 1974.
8. N.Z. Cho and C.J. Park, "A Wavelet-Based Image Reconstruction in Transmission Computed Tomography," *Proceedings of 1998 ANS Radiation Protection and Shielding Division Topical Conference*, **Vol. 2**, p.141, Nashville, U.S.A., April 1998.
9. C.J. Park and N.Z. Cho, "Image Reconstruction in Emission Computed Tomography vi Multigrid Wavelet-Based Natural Pixel Method," *Proceedings of International Conference on the Physics of Nuclear Science and Technology, Long Island, New York (October 1998) (to be presented).*
10. G. Beylkin, et al., "Fast Wavelet Transforms and Numerical Algorithms," *Comm. Pure. Appl. Math.,* **43**, 141-183, 1991.